CNWRA *A center of excellence in earth sciences and engineering*

A Division of Southwest Research Institute™
6220 Culebra Road • San Antonio, Texas, U.S.A. 78228-5166
(210) 522-5160 • Fax (210) 522-5155

November 2, 2000
Contract No. NRC-02-97-009
Account No. 20.01402.571

U.S. Nuclear Regulatory Commission
ATTN: Mrs. Deborah A. DeMarco
Two White Flint North
11545 Rockville Pike
Mail Stop T8 A23
Washington, DC 20555

Subject: Programmatic review of a paper

Dear Mrs. DeMarco:

Enclosed is a paper entitled "The Critical Potential for the Stress Corrosion Cracking of Fe-Cr-Ni Alloys and its Mechanic Implications," to be presented at The Minerals, Metals and Materials Society (TMS) symposium "Chemistry and Electrochemistry of Corrosion and Stress Corrosion: A Symposium to Honor the Contributions of Professor Roger W. Staehle" to be held on February 11–15, 2001 in New Orleans, LA. The paper presents a critical discussion of mechanistic and empirical models of stress corrosion cracking (SCC) and describes experimental results reported in the literature, as well as those resulting from our own work. It is shown that the critical potential for SCC is equivalent to the repassivation potential for crevice corrosion for Fe-Cr-Ni-Mo alloys containing less than 45% Ni. It is concluded, however, that none of the current mechanistic models offers a good explanation for the existence of the critical potential. The discussion regarding this potential and the threshold stress intensity is relevant to the long-term prediction of SCC for HLW container materials.

Please advise me of the results of your programmatic review, so that we can submit the paper for publication in a timely manner. If you have any questions regarding this paper, please feel free to contact Gustavo Cragnolino at (210) 522-5539.

Sincerely yours,

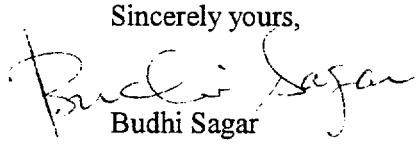

Budhi Sagar
Technical Director

BS:NS:jg

Enclosure

cc:	J. Linehan	T. Bloomer	B. Leslie	CNWRA EMs	T. Nagy (contracts)
	T. Ahn	C. Greene	J. Andersen	CNWRA Dirs:	
	B. Meehan	K. Stablein	W. Patrick	D.S. Dunn	
	E. Whitt	J. Greeves	Y. Pan	P. Maldonado	
	J. Thomas	J. Holonich	G. Cragnolino		

Washington Office • Twinbrook Metro Plaza #210
12300 Twinbrook Parkway • Rockville, Maryland 20852-1606

THE CRITICAL POTENTIAL FOR THE STRESS CORROSION CRACKING OF Fe-Cr-Ni ALLOYS AND ITS MECHANISTIC IMPLICATIONS

G.A. Cragnolino, D.S. Dunn, Y.M. Pan and N. Sridhar

Center for Nuclear Waste Regulatory Analyses (CNWRA)
Southwest Research Institute
San Antonio, TX 78238-5166

Abstract

Since the concept of a critical potential for the transgranular stress corrosion cracking (SCC) of austenitic stainless steel (SS) in hot, concentrated chloride solutions was introduced in the 1970s, several mechanisms have been suggested and discussed in the literature. SCC of Fe-Cr-Ni alloys has been interpreted in terms of hydrogen-induced cracking, adsorption-induced cleavage, slip dissolution/film rupture, film-induced cleavage, and surface mobility, as well as variations of these mechanisms. In this paper we review briefly some of these mechanisms and discuss the existence of a critical potential on the bases of experimental results reported in the literature for Fe-Cr-Ni alloys and our own work using alloys with different Ni contents, such as type 316L SS (Fe-18Cr-12Ni-2.5Mo), alloy 825 (42Ni-29Fe-22Cr-3Mo) and alloy 22 (58Ni-22Cr-13Mo-4Fe-3W), in concentrated chloride solutions at temperatures ranging from 95 to 120 °C. We conclude that the existence of this potential, although valid for alloys containing less than ~42% Ni within certain ranges of chloride concentrations and temperatures, cannot be interpreted in support of any of the discussed mechanisms. The relationship of this critical potential with the repassivation potential for localized corrosion is discussed.

Introduction

Thirty years ago, in a series of papers on the transgranular stress corrosion cracking (SCC) of austenitic stainless steels (SSs) in hot, concentrated $MgCl_2$ solutions, Uhlig and coworkers[1,2] reported that SCC did not occur at potentials lower than a critical potential. These results confirmed previous findings of several authors[3-6]. Uhlig concluded[7,8] that under natural corroding conditions SCC would occur only if the corrosion potential, E_{corr}, was higher than a critical potential, which depends on the specific metal/environment system. Although Uhlig only discussed the critical potential in support of his proposed mechanism of adsorption-induced SCC[7,8], several alternative mechanisms had been proposed at that time, as discussed by Staehle[9,10] after conducting an extensive and detailed review of the SCC literature on Fe-Cr-Ni alloys[11,12]. The SCC of austenitic Fe-Cr-Ni alloys in chloride solutions had mainly been interpreted in terms of hydrogen-induced cracking, adsorption-induced cleavage, and slip dissolution/film rupture, as well as variations of these mechanisms. Staehle[9,10] dismissed both the hydrogen- and adsorption-induced cracking mechanisms and provided carefully drawn arguments and indirect experimental evidence in support of the slip dissolution/film rupture mechanism.

In the last 20 years, a significant effort has been made to provide a quantitative basis to the slip dissolution/film rupture model[13,14], while alternative SCC mechanisms such as film-induced cleavage[15], and surface mobility[16] have been postulated. During the same period, extensive experimental work on the SCC of austenitic Fe-Cr-Ni alloys in chloride solutions has been reported in the literature, as reviewed by Newman and Mehta[17] and others[18,19]. One of the most important observations, in this regard, arises from the work of Tsujikawa and coworkers[20,21] showing that a critical potential, corresponding to the repassivation potential for crevice corrosion, also exists for the SCC of several Fe-Cr-Ni alloys in dilute, neutral chloride solutions.

In this paper, we discuss the validity of the critical potential concept on the bases of experimental results reported in the literature for fcc Fe-Cr-Ni alloys, in particular those containing Mo, and our own work using alloys with different Ni contents, such as type 316L SS (Fe-18Cr-12Ni-2.5Mo), alloy 825 (42Ni-29Fe-22Cr-3Mo) and alloy 22 (58Ni-22Cr-13Mo-4Fe-3W), in chloride solutions of various concentrations at temperatures ranging from 95 to 120 °C. We also discuss the main assumptions and results derived of the slip dissolution/film rupture[13,14], film-induced cleavage[15], and surface mobility[16] mechanisms and some of the difficulties confronted in attempting to apply these mechanisms to predict the SCC of Fe-Cr-Ni alloys in chloride solutions. For this purpose a brief description of those models is included in the following section, as well as a summary of a more empirical approach using fracture mechanics concepts. Satisfactory modeling of SCC and experimental evaluation of critical parameters are required in many industrial applications, particularly when long-term performance is expected as in the case of high-level radioactive waste containers.

Stress Corrosion Cracking Models

Mechanistic Models

From the experimental determination of the effects of the main variables affecting the initiation and propagation of cracks, such as the nature and concentration of the chemical species present in the environment, either as active cracking promoters (C_A) (e.g., Cl^- for austenitic SSs) or as cracking inhibitors (C_{Inh}) (e.g., CrO_4^{2-} for the caustic cracking of SSs), potential (E), temperature (T), pH, stress (σ), etc., it is expected that the failure time, t_f, can be expressed by a functional relationship between these variables.

$$t_f = f\left(C_A, C_{Inh}, T, E, pH, \sigma, \ldots\right) \quad (1)$$

where t_f is given by

$$t_f = t_i + t_p \quad (2)$$

with t_i as the initiation or induction time and t_p as the crack propagation time. In principle, the final purpose of any mechanistic modeling of SCC is to develop a similar type of relationship through mathematical modeling using fundamental electrochemical and mechanical laws and equations.

In many SCC failures, there is indirect evidence that the initiation stage is the dominant term in the lifetime of the component. However, the initiation stage has not been extensively investigated, mainly due to experimental difficulties involved in the detection of a crack nucleus prior to noticeable growth and the stochastic nature of crack initiation in single phase, non-sensitized alloys. Therefore, very limited attempts have been made to model crack initiation. Using linear-elastic fracture mechanics (LEFM), Hagn[22] has computed a critical threshold crack size, a_{th}, for both SCC and corrosion fatigue (CF). The equation used to define a_{th} is applicable, however, to crack sizes greater than 80 μm, which is a value almost an order of magnitude larger than the minimum depth (or length) usually reported in the literature for actively growing cracks. In addition, no consideration was given to the electrochemical or environmental factors involved in the initiation of SCC. An attempt has been made[23,24] to include electrochemical factors by using a crack-tip opening displacement (CTOD) model based on LEFM concepts and assuming the anodic process of crack initiation under activation control. The initiation time was expressed as

$$t_i = \frac{K_{Iscc}^2}{\pi B(\sigma^2 - \sigma_0^2)} \exp\left(\frac{-\beta F\left(E - E_{corr}\right)}{RT}\right) \quad (3)$$

where K_{Iscc} is the threshold stress intensity for SCC, σ the applied stress, σ_0 the stress necessary to close the crack nucleus, β the transfer coefficient for the anodic reaction, and E the potential, whereas B is given by the following equation

$$B = \left(\frac{M}{zF\rho}\right) i_{corr} \quad (4)$$

where M is the atomic weight, ρ the density, and i_{corr} the corrosion current density. Although the model provides an analytical relationship between t_i and both mechanical (σ) and electrochemical (E) variables, significant discrepancies were found[24] between the values of B and β calculated from the current density versus potential plots and those computed from the measured values of t_i using Eqs. (3) and (4). These discrepancies should be expected, leaving aside the simplistic description of the electrochemical process, by the limitations of LEFM to deal with small size cracks.

Contrary to what happens regarding crack initiation, many mechanistic models have been proposed to address crack propagation. As noted by Parkins[25,26] and Jones and Ricker[27], it is unlikely that a single mechanism for SCC exists. Leaving aside mechanisms determined by cathodic processes such as hydrogen embrittlement, which seems inapplicable to chloride-induced SCC of austenitic Fe-Cr-Ni alloys, some models have evolved in recent years to address SCC promoted by anodic processes in which an

expression for the crack velocity in terms of environmental, electrochemical, or mechanical parameters has been developed.

Slip-Dissolution Model The slip-dissolution model is probably one of the most quoted models to explain the SCC behavior of ductile alloys. In its most simple expression, which has been termed an "electrochemical knife" by Beck[28], the crack velocity, v, is derived from Faraday's laws according to an expression similar to Eq. (4), in which

$$v = \left(\frac{M}{zF\rho}\right) i_{tip} \tag{5}$$

where i_{tip} indicates the current density at the crack tip which is assumed to be a bare metal. The high aspect ratio of the crack is preserved because the crack walls are assumed to be almost instantaneously repassivated by the formation of a protective film, and the role of stress is merely to open the crack sides allowing the solution to reach the crack tip. Many methods for measuring transient currents on bare surfaces, including scratching, scraping, fast straining, fast fracture, etc., have been used to determine i_{tip}[29,30]. However, controversy exists about the simulation of the environment present at the crack tip, the correction for the potential drops expected in fast transients, and the approximations involved in the calculation of the reactive area[31].

Many attempts were made to modify Eq. (5), by considering separately the electrochemical and mechanical factors operating at the crack tip that may determine the value of the crack velocity. Whereas continuous anodic dissolution is implicitly assumed in Eq. (5), several authors[9,10,32-37] and more recently Ford[13] suggested a discontinuous anodic process caused by film formation, rupture of the film by slip-step emergence, dissolution at slip-steps, and reformation of the film in a repetitive sequence. Leaving aside an analysis of the differences between these models, expressions presented by Ford and Andresen[38] illustrate the role of the electrochemical and mechanical factors. They assumed that at the crack tip, the metal dissolution rate on a bare surface, i_{tip}, can be maintained over a time, τ_0, before the current density decreases because of film formation. If the metal is stressed, the strain in the growing film will increase with time. Once the strain exceeds the fracture strain of the film, ε_f, the dissolution/repassivation process will repeat itself with a periodicity, τ_f, defined by the ratio $\varepsilon_f / \dot{\varepsilon}_{tip}$, where $\dot{\varepsilon}_{tip}$ is the strain rate at the crack tip. Therefore, if $\tau_f \gg \tau_o$, Eq. (5) can be modified resulting in

$$v = \left(\frac{M}{zF\rho}\right)\left(\frac{i_{tip}}{1-n}\right)\left(\frac{\tau_0 \dot{\varepsilon}_{tip}}{\varepsilon_f}\right)^n \tag{6}$$

which is reduced to Eq. (5) for the limiting case in which τ_f is less than τ_o and $n \rightarrow 0$ meaning that the crack tip is maintained as a bare surface. Although it is predicted that i_{tip}, τ_o, n, and ε_f can be independently determined by electrochemical techniques using straining electrodes or other methods, in general the predicted values do not correspond with the experimentally measured crack growth rates. Therefore, Eq. (6) has been reformulated[13,38] as

$$v = A(\dot{\varepsilon}_{tip})^n \tag{7}$$

where A and n are postulated to be constants depending on certain properties of the material (i.e., degree of sensitization) and the environment (i.e., solution conductivity) that were empirically determined on the basis of extensive experimental work conducted on sensitized type 304 SS in oxygenated water systems typical of the environments prevailing in BWRs[39]. However, one of the main limitations in the application of Eq. (7) is that $\dot{\varepsilon}_{tip}$ cannot be directly measured. Several authors[40-42] have developed or reviewed empirical or theoretical formulations of $\dot{\varepsilon}_{tip}$ in terms of macroscopic stress or strain variables. Considerable uncertainty exists regarding the validity of these formulations. The empirical relationships used by Ford[42] for type 304 SS are

$$\dot{\varepsilon}_{tip}(s^{-1}) = 4.1x10^{-4} K^4 \tag{8}$$

for constant loading where the stress intensity factor, K, is expressed in MPa·m^{½}, and

$$\dot{\varepsilon}_{tip}(s^{-1}) = 10\ \dot{\varepsilon}_{app} \tag{9}$$

for constant applied strain rate, $\dot{\varepsilon}_{app}$, in s^{-1}.

Although the slip-dissolution model was initially applied to the transgranular SCC (TGSCC) of austenitic SSs in hot, acidic chloride solutions, it is increasingly viewed as primarily associated with intergranular SCC (IGSCC) of sensitized Fe-Cr-Ni alloys, in which a preexisting path for anodic dissolution exists. However, Ford and Andresen[14] have extended the application of the model to a variety of alloy systems including pressure vessel steels (ASTM A533/A508), austenitic SSs (304/316L), and nickel-base alloys (600/182) in high-temperature (~300 °C) aqueous environments. For this purpose, empirical correlations have been developed on the basis of a combination of laboratory experimental results and field observations. Using a simplified expression of the stress intensity factor, K, given by

$$K = Y\sigma(\pi a)^{1/2} \tag{10}$$

where Y is a geometric factor and a is the crack size, the dependence of a with time can be calculated. From the analysis of the extensive work conducted by Ford and Andresen[14], it can be concluded that most of the final expressions for calculating crack growth rates and crack depth require the input of field data in order to adjust several of the parameters included in the model. This is particularly true in the case of the parameter n as expressed in Eq. (7).

Macdonald and Urquidi-Macdonald[43,44] have questioned the electrochemical basis of the slip-dissolution model as formulated by Ford and Andresen, by stating that the model does not account for the conservation of charge. By coupling the cathodic reactions occurring on the passive surfaces with the metal dissolution at the crack tip, they claimed that the control of the crack growth rate may switch from the crack internal environment to the external environment, depending upon the increase in the resistivity of the solution and the kinetics of the reduction reaction. These diverging interpretations, among other aspects, have been the subject of an open controversy[45-47] which cannot be covered in this brief review. However, apart from those considerations, Macdonald and Urquidi-Macdonald[43,44] also assumed that slip-dissolution is the basic mechanism for crack advance.

In their model[44,48], the crack growth rate is calculated also with an expression based on Faraday's laws

$$v = \left(\frac{M}{zF\rho}\right)\left(\frac{I_0}{2A_{crack}}\right) \tag{11}$$

where A_{crack} is the area of the crack mouth and I_0, the current averaged over the slip dissolution/repassivation cycle, is given by:

$$I_0 = 2i_0^0 A_{tip}\left(\frac{\tau_0}{\tau_f}\right)^{1/2} \exp\left[-\frac{(\phi_s^L - \phi_s^0}{b_a}\right] \tag{12}$$

where i_0^0 is the standard exchange current density for the dissolution reaction, A_{tip} the crack tip area, τ_0 a constant derived from the repassivation transient, τ_f the time of cyclical fracture of the passive film at the crack tip, ϕ_s^L the potential in the solution adjacent to the crack tip, ϕ_s^0 the standard potential, and b_a the Tafel constant. The same problems, described above for the definition of the crack tip strain rate, are also encountered in this model. In particular, no threshold value for K below which SCC does not occur can be defined and crack growth rate seems to increase almost continuously with K up to relatively high K values (~50 MPa·m^{½}) without exhibiting any transition to the characteristic plateau.

Film-Induced Cleavage Model The high crack growth rates observed in certain cases of TGSCC, which cannot be explained in terms of bare-surface current densities, as well as the apparent discontinuous crack advance events, which are observed as distinctive crack arrest markings on fracture surfaces, are difficult to reconcile with a model based on slip dissolution. This led to the postulation of environmentally induced cleavage as an alternative crack advance mechanism.[49] Sieradzki and Newman[15] have developed the concept that cracks initiated in brittle, thin films formed by anodic reaction at the crack tip could propagate by cleavage over distances of a few microns in the ductile substrate. It is beyond the scope of this review to provide a detailed discussion of the electrochemical and mechanical factors involved in the development of this model. Turnbull[50] has critically reviewed most of the experimental evidences for and against this model. Atomistic calculations and computer simulations have been presented in support of the model. However, few attempts have been made toward establishing quantitative expressions for crack propagation rate.

Parkins[26] considered the time interval between the repetitive events of film growth and crack jumping (essentially, the time to grow the film since the jump is assumed to be almost instantaneous) as that required to reach the critical strain for crack initiation in the film, ε_c. This time is strain-rate dependent and equal to $\varepsilon_c / \dot{\varepsilon}$. Therefore, the crack velocity is defined as

$$v = (l + j)\frac{\dot{\varepsilon}}{\dot{\varepsilon}_c} \tag{13}$$

where l is the film thickness and j is the jump distance in the cleavage event. In contrast, Cole et al.[51] expressed the crack growth rate as

$$v = \left(\frac{M}{zF\rho}\right)\frac{Q_\tau}{\tau} \tag{14}$$

where Q_τ is the anodic charge density passed during the interval, τ, between successive cleavage events (calculated from the spacing between arrest markings divided by the crack velocity). The main limitation of both Eqs. (13) and (14) is that they cannot be used for predicting crack growth rates because parameters only accessible through fractographic or metallographic observation of failed specimens are required. It is also difficult to conceive that the size of the cleavage step is not influenced by modifications in mechanical conditions, such as stress or strain.

Surface Mobility Model The surface mobility model developed by Galvele[16] is not specific to anodic cracking processes but is claimed to be applicable to SCC (with the exception of alloys exhibiting a preexisting susceptible path), liquid metal embrittlement, and hydrogen embrittlement of nonhydride-forming metals. The crack propagation results from the capture of vacancies by the stressed lattice at the tip of the crack. The rate-controlling step is the rate of movement of excess ad-atoms and, in turn, vacancies along the surface of the crack; the role of the environment is to change the surface self-diffusivity of the metal or alloy. The mechanism predicts that SCC should be observed on tensile-stressed metals at temperatures below 0.5 T_m (T_m is the melting point of the metal in K), under environmental conditions that promote high surface mobility. In particular, this can occur when a contaminant that enhances surface diffusion is chemi-adsorbed on a metal surface. According to Galvele[52], the environment also assures a free supply of vacancies to the metal surface by selective dissolution of the alloy or by film growth processes dominated by movement of cation vacancies.

In this model, crack velocity for SCC based on anodic processes is given by

$$v = \frac{D_s}{L}\left[\exp\left(\frac{\sigma a^3}{kT}\right) - 1\right] \tag{15}$$

where D_s is the coefficient of surface self-diffusion, L the diffusion path of the ad-atoms or vacancies (typically 10^{-8} m), σ the maximum stress at the crack tip, a the atomic distance, k the Bolztmann constant, and T the absolute temperature. With the exception of a few specific cases, the value of D_s is not readily measurable but can be estimated by using approximate expressions[16].

This model is highly controversial, and Turnbull[50] has raised objections to the use of thermodynamically based equations for the calculations of vacancy concentrations, as well as some of the approximations used by Galvele. Nevertheless, the model has been applied by Galvele and coworkers to the prediction of crack velocity for several alloy/environment systems with reasonable success[53-56].

Empirical Models

The application of LEFM concepts to the study of SCC, pioneered by Brown[57], led to the possibility of establishing quantitative, though empirical, relationships between crack velocity and the effective tensile stress acting at the crack tip, as defined by the stress intensity factor, K. For the opening mode (Mode I), the associated K is then defined as K_I, according to expressions similar to Eq. (10), in which Y is a parameter that depends on the specimen and crack geometries, and the loading configuration. Many alloy/environment systems exhibit, at least partially, the dependence between the logarithm of crack velocity

and K_I depicted schematically in Figure 1. Subcritical crack growth occurs in the stress-dependent part (Stage I) at a rate that usually increases exponentially with K_I, above the threshold stress intensity for SCC, K_{Iscc}, an environment-dependent parameter. On the contrary, the critical stress intensity, K_{Ic} (commonly termed fracture toughness) is an intrinsic material property. The crack velocity in Stage I can be expressed as

$$v_I = v_o \exp[c_1(K_I - K_{Iscc})] \tag{16}$$

where v_o is the minimum crack velocity that can be measured, corresponding to K_{Iscc}. Values of c_1 ranging from 0.5 to 3 $(MPa \cdot m^{1/2})^{-1}$ were reported by Speidel[58] for aluminum alloys in aqueous solutions. For SSs, c_1 values are probably close to the upper limit of that range.

However, it is difficult to obtain accurate velocity data in Stage I. Jones and Simonen[59] have suggested that a Paris-type relationship, as observed under cyclic loading, could also be applicable to Stage I growth. Hence, crack velocity can be expressed as

$$v_I = c_1^* K_I^m \tag{17}$$

where $c_1^* = v_o / K_{Iscc}^m$. Jones and Simonen[59] reviewed data obtained by many authors for a variety of materials and experimental conditions and found that m varied from values as low as 2 for brass to up to 24 for SSs, with most of the values for steels above 5. They found that several models were unsatisfactory to explain the dependence expressed by Eq. (17), concluding that m depends on the CTOD and the local crack-tip chemistry, and presented a model based on crack velocity controlled by electromigration of Ni^{2+} cations through a porous salt film for Stage I of the IGSCC of P-doped Ni in a H_2SO_4 solution.

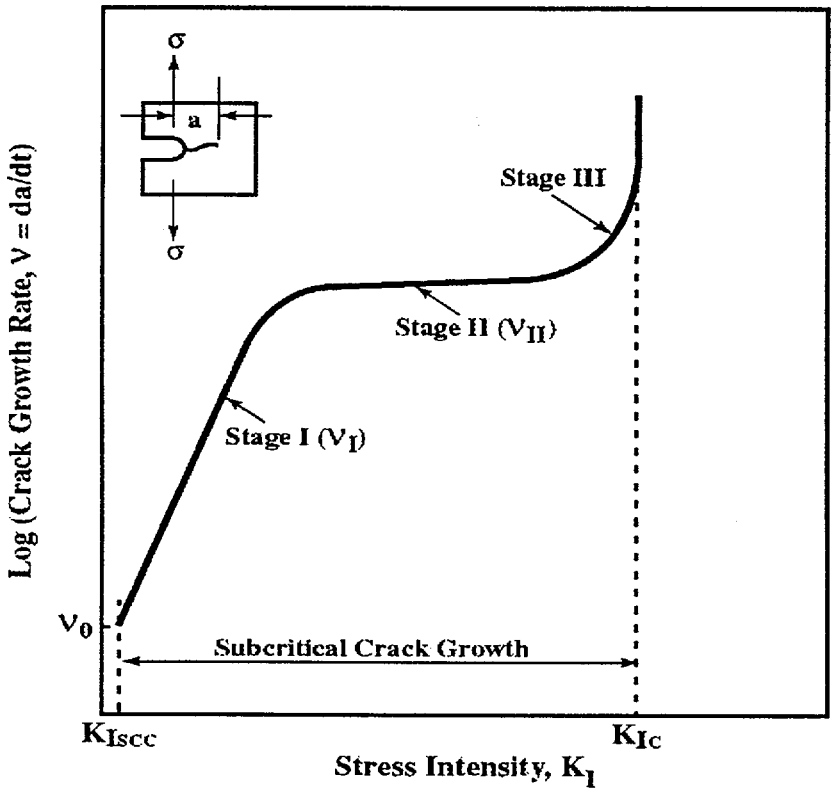

Figure 1: Schematic curve of crack velocity as a function of stress intensity showing the stages of crack propagation.

Although K_{Iscc} is defined as a threshold or minimum stress intensity below which an existing crack will not grow, a conventional crack velocity limit is adopted for the definition of K_{Iscc}. Speidel[60], investigating the SCC of a variety of Fe-Cr-Ni alloys in concentrated chloride solutions at boiling temperatures, adopted a minimum velocity, v_o, of 3×10^{-11} m/s. However, v_o can be

reduced to values lower than 3×10^{-13} m/s by using extended testing times (at least 1 yr) or improved techniques for measuring crack extension, able to detect a crack advance far shorter than 1 μm[61].

The crack velocities measured in the almost stress-independent part of the curve in Figure 1 (Stage II) range from 10^{-11} to 10^{-6} m/s for a variety of alloys in aqueous solutions, depending also on metallurgical and environmental conditions. Speidel[58] has suggested empirical expressions for the crack growth rate in Stage II that require further evaluation. The effect of the concentration of aggressive anions can be expressed as

$$v_{II} = v_{II}(0) + c_2 C_A^n \tag{18}$$

where v_{II} is the plateau crack growth rate, $v_{II}(0)$ the crack growth rate at very low concentrations of the aggressive anion, c_2 a constant, C_A the concentration of the aggressive anion, and n an exponent ranging from 0.33 to 1

The effect of temperature on crack growth rate in Stage II is given by

$$v_{II} = v_{II}^0 \exp(-E_a / RT) \tag{19}$$

where E_a is the apparent activation energy. For certain alloy/environment systems (e.g., aluminum-base and titanium-base alloys in chloride-containing solutions), it has been observed[58,62] that E_a ranges from 18 to 23 kJ/mole. This range of values seems to indicate that the crack growth in Stage II is mainly controlled by diffusional processes in aqueous solutions for which typical values for several electrolytes (e.g., NaCl, $CaCl_2$, HCl, and NaOH) are approximately 10 to 12 kJ/mole[63]. However, Russell and Tromans[64] found for 25 and 50% cold-worked type 316 SS in hot, concentrated $MgCl_2$ solutions a value of E_a equal to ~65 kJ/mole. This value led them to suggest that the rate-controlling steps in SSs seem to be dominated by chemisorption or kinetic effects, including electrochemical dissolution and repassivation.

The crack growth rate in Stage I is also dependent on temperature and Speidel[58] has suggested an expression for this dependance of the crack velocity. The value of E_a in Stage I for aluminum alloys in chloride solutions is approximately 110 kJ/mole[58], which is almost an order of magnitude larger than that for Stage II. A similar value was reported for a titanium alloy in 10 M HCl solution[65]. These high values suggest that mechanical factors related to the CTOD, defined as $K_I^2/\sigma_y E$, predominate in controlling the crack growth rate in Stage I.

Experimental Evidence of the Existence of a Critical Potential

Once a crack is initiated, propagation, even at velocities in the lowest end of the range that can be measured in Stage I (i.e., 3×10^{-11} m/s), will lead to failure of components expected to have a long lifetime, unless a crack arrest mechanism can be postulated. This is the case of metallic containers for the geological disposal of high-level radioactive waste for which a performance period of many thousand years is expected[73]. It can be concluded in these cases that any attempt to use an empirical model for predicting the occurrence of SCC as a failure process should rest on predicting the environmental and electrochemical conditions that would avoid crack initiation or eventually would lead to crack arrest.

Relevant Results Reported in the Literature

Although limited, in comparison to crack growth rate data for Stage II, there are experimental results showing that K_{Iscc} is affected by the electrode potential. Eremias and Marichev[66] demonstrated that an increase in potential of about 350 mV, with respect to the E_{corr} (−400 mV_{SCE}), decreases K_{Iscc} from 12 to 2 MPa·$m^{½}$ for an austenitic SS (Fe-18Cr-10Ni-0.5Ti) in concentrated (10.8 molal) LiCl solution at 105 °C. A cathodic overpotential of 50 mV, on the other hand, increased K_{Iscc} up to 16 MPa·$m^{½}$. Concurrently, there was a pronounced increase of v_I (more than an order of magnitude) under an anodic overpotential of 50 mV. Russell and Tromans[64] did not observe an effect of potential on the Stage II crack velocity at K_I greater than 20 MPa·$m^{½}$ for type 316L SS in hot, concentrated $MgCl_2$ solution at temperatures ranging from 116 to 154 °C. At the E_{corr} the crack growth rate was 6×10^{-8} m/s at 116 °C and increased to 4×10^{-7} m/s when the temperature was increased to 154 °C. At this temperature, the Stage II crack velocity was independent of potential at potentials higher than −325 mV_{SCE}. However, the application of a potential 50 mV lower than the E_{corr} (−300 mV_{SCE}) led to crack arrest.

Although Silcock[67] used smooth uniaxial tensile specimens rather than precracked fracture mechanics specimens, her studies of the TGSCC of type 316 SS in boiling 42 % $MgCl_2$ solutions at 154 °C clearly show the dominant effect of potential in crack nucleation and growth. Curves rather similar to that of Figure 1 for Stages I and II were obtained by plotting crack velocity as a function of the nominal applied stress for various applied potentials. Cracks were initiated at a stress of 60 N·m^{-2} at −280 mV_{SCE}, whereas a stress of 200 N·m^{-2}, higher than that obtained by extrapolating the data at intermediate potentials, was required to nucleate cracks at −340 mV_{SCE}, suggesting that cracks cannot be initiated in this severe environment at potentials lower than −340 mV_{SCE}. Other authors[49,68,69], using constant load or slow strain rate tests, have also reported the existence of a critical potential for the TGSCC of type 304 SS in hot concentrated LiCl solutions, as well as the potential dependence of the crack growth rate.

Difficulties associated with the initiation of cracks in dilute, neutral chloride solutions at temperatures around 100 °C or less are reflected in the scarce number of papers dealing with the effect of potential under such environment conditions[19]. In a series of papers, Tsujikawa and coworkers[20,21] clearly demonstrated that the specific environmental requirements to initiate SCC of Fe-Cr-Ni alloys in chloride solutions are attained in a geometrically creviced area. Crack initiation and propagation was observed in creviced and tapered double cantilever beam (DCB) specimens of type 316 SS exposed to dilute (0.005 to 0.5 M) NaCl solutions at 80 °C and K_I greater than 4 MPa·$m^{½}$ by applying a potential 10 mV higher than the repassivation potential, E_{rp}, for crevice corrosion. Critical potentials for SCC were also determined for a set of fifty two Fe-18Cr-14Ni alloys with varying P, Cu, Mo, and Al contents using specimens in which a crevice is formed and residual stresses are induced by spot welding together two flat pieces of the steels[70].

Our Experimental Results

During the course of our work evaluating the corrosion resistance and the long-term performance of candidate container materials for high-level radioactive waste disposal, using several techniques such as slow strain rate, constant deflection, and fracture mechanics tests, we studied the SCC susceptibility of various fcc Fe-Cr-Ni-Mo alloys covering a wide range of Ni contents. The alloys studied include type 316 L SS (Fe-18Cr-12Ni-2.5Mo), alloy 825 (42Ni-29Fe-22Cr-3Mo) and alloy 22 (58Ni-22Cr-13Mo-4Fe-3W) exposed to chloride-containing environments at temperatures around 100 °C. A summary of results already reported[71,72] are presented below and complemented with updated information.

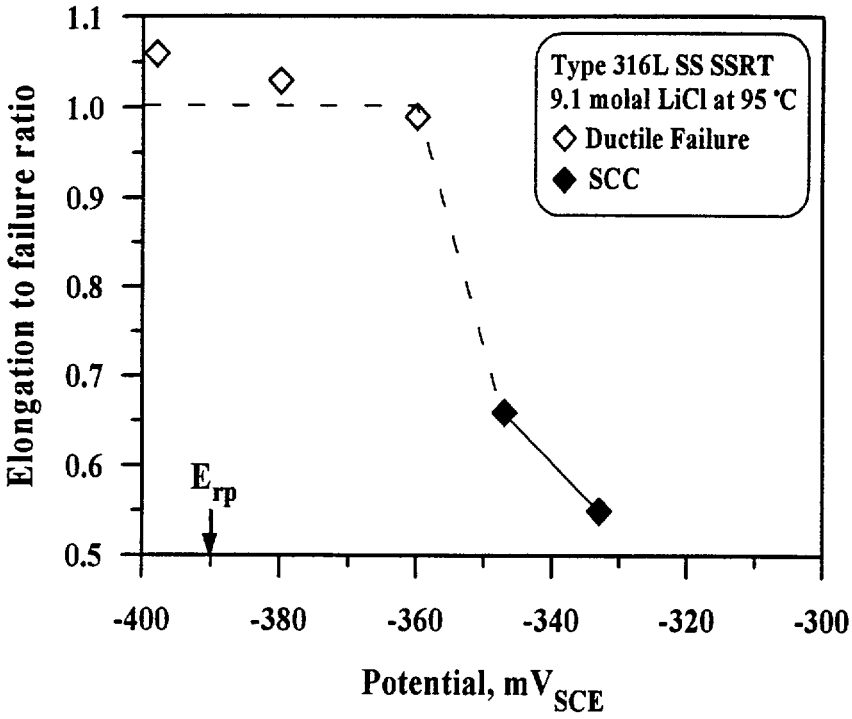

Figure 2: Effect of potential on the elongation to failure ratio for type 316L SS in LiCl solution. E_{rp} denotes the repassivation potential in the solution.

Slow Strain Rate Tests Slow strain rate tests for type 316 L SS at initial strain rates ranging from 1.0×10^{-6} to 2.0×10^{-7} s^{-1} were conducted using smooth round tensile specimens in various concentrated chloride solutions at temperatures ranging from 95 to 120 °C. Figure 2 shows the results obtained in one of these sets of tests. The elongation to failure ratio (elongation to failure in solution to that in an inert environment at the same temperature) is plotted as a function of applied potential for tests conducted at 95 °C in 9.1 molal LiCl solution acidified to pH 4.0 by the addition of HCl. An increase of the potential above E_{rp} (measured at the same temperature using cyclic potentiodynamic polarization tests with unstressed specimens) induced a significant decrease in the elongation to failure ratio, indicating the occurrence of SCC.

Figure 3 summarizes the results of slow strain rate tests obtained in chloride solutions with different cations by plotting the potential versus the chloride concentration. The solutions include a near saturation 6.4 molal NaCl (without and with the addition of 0.01 M $Na_2S_2O_3$) at 95 °C; 6.4 to 14.0 molal LiCl at 95, 110, and 120 °C; 9.1 molal Cl^- (as $MgCl_2$) at 110 °C and 14.0 molal Cl^- (as $MgCl_2$) at 120 °C. Confirming results in the literature, SCC was observed at both temperatures in $MgCl_2$ solutions at the E_{corr} and at a small anodic overpotential, but no SCC was found at 95 °C in NaCl and LiCl solutions at a concentration of 6.4 molal, even when the solutions were acidified to pH 2.6. However, SCC was observed at concentrations higher than 7.2 molal in LiCl solutions acidified to pH 4.0, which is a pH close to that attained by $MgCl_2$ as a result of cation hydrolysis. SCC

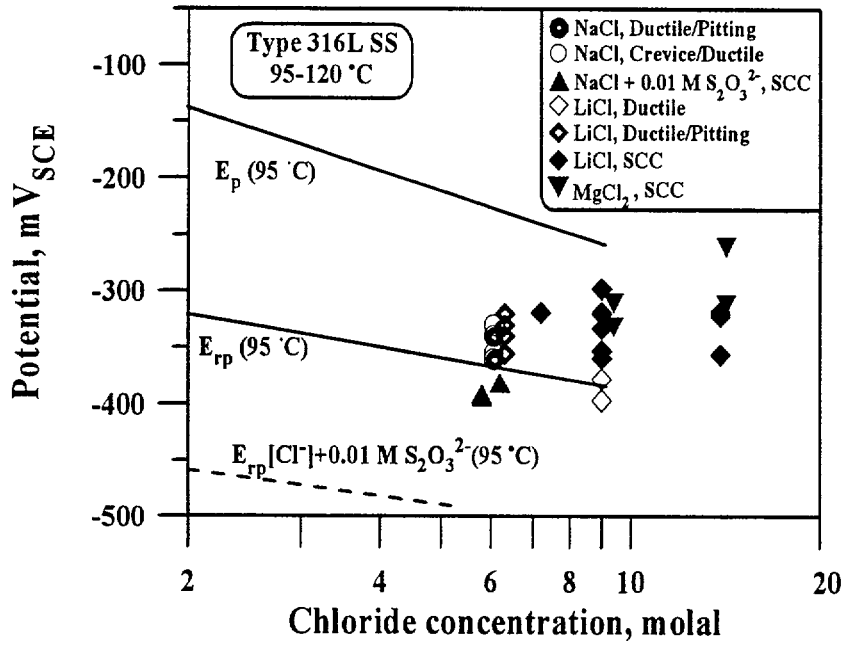

Figure 3: Slow strain rate test results for type 316L SS in various chloride solutions. E_p and E_{rp} denote the pit initiation potential and the repassivation potential.

only occurred in 6.4 molal NaCl solution at 95 °C in the presence of $Na_2S_2O_3$.

The most relevant observation from these tests is that for SCC to occur, in addition to the requirement of a minimum chloride concentration, the potentials must be higher than E_{rp}. No tests were conducted at potential above the pitting nucleation potential, E_p, to avoid the occurrence of generalized pitting instead of the initiation and growth of cracks. Although it seems that SCC occurred at potentials lower than E_{rp} in the presence of $Na_2S_2O_3$, it should be noted in Figure 3 that E_{rp} is lowered by the addition of $Na_2S_2O_3$ to the NaCl solution. Even in the presence of $Na_2S_2O_3$, a minimum chloride concentration is required to induce SCC in slow strain rate tests. Thus, ductile failure accompanied by minor localized corrosion was observed in 0.0028 molal NaCl above E_{rp}.

As expected, alloy 825 was found to be significantly more resistant to SCC in chloride solutions than type 316L SS under similar experimental conditions. No cracking was detected in tests conducted using smooth or notched tensile specimens at two anodic potentials above E_{rp} in 9.1 molal LiCl solution (pH 4.0) at 95 °C, neither in 5.8 molal NaCl with the addition of 0.01 M $Na_2S_2O_3$ at the same temperature. Only ductile failure accompanied by pitting corrosion was observed in both solutions. SCC was only detected in 14.0 molal Cl^- (as $MgCl_2$) solution at 120 °C. Using specimens with a PTFE device to create a tight crevice in the gauge section, SCC was promoted both in the 9.1 molal LiCl solution as well as in the 5.8 molal NaCl solution containing $Na_2S_2O_3$ (Figure 4). It appears that the chloride concentration increased inside the occluded cell formed by the crevice, leading to the initiation and growth of transgranular cracks.

Constant Deflection Tests Constant deflection tests were conducted using U-bend specimens of type 316L SS and alloy 825 immersed partially in the solution such that the legs of the U-bend were in the vapor space while the apex was submerged completely in the solution. The maximum test duration was 1,848 hr. Contrary to the results of the slow strain rate tests, SCC was observed in type 316 L SS above E_{rp} even in the dilute NaCl solution (0.028 molal) at 95 °C. Cracking was found to be more severe in the presence of $Na_2S_2O_3$. Cracks were found above the vapor/solution interface despite the fact that the legs were the less stressed part of the U-bend specimens. Although no systematic testing was conducted in this case at potentials below E_{rp}, all tests showed in a relatively conclusive manner the occurrence of SCC in a range of potentials above E_{rp} within which generalized pitting did not occur.

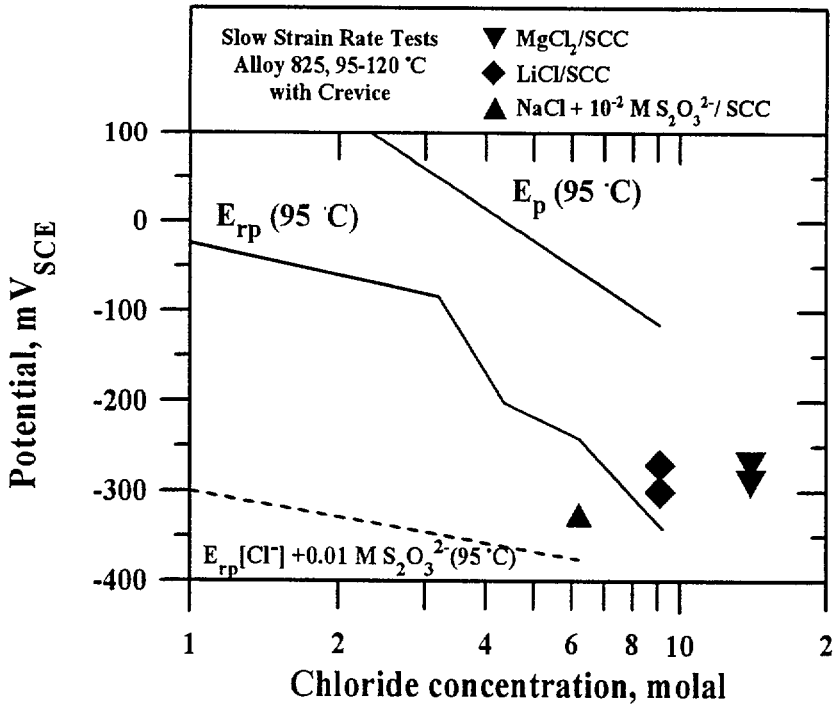

Figure 4: Slow strain rate test results for creviced specimens of Alloy 825 in various chloride solutions

No cracks were initiated in single and double U-bend specimens of alloy 825 under equivalent testing conditions, at potentials above and below E_{rp}, in some cases over a total test time of 4,536 hr (189 days).

Even in 5.8 molal NaCl or 9.1 molal LiCl solutions, no SCC was detected. At anodic potentials, both in NaCl and in LiCl solutions, pits were detected after 504 h (21 days) above the vapor/solution interface but the pits did not give rise to cracks upon further exposure to the solution.

Fracture Mechanics Tests These tests were conducted using three types of precracked fracture mechanics specimens. They are double cantilever beam (DCB), modified wedge-opening-loaded (WOL), and compact tension (CT) specimens. These specimens were machined from plates of both type 316L SS and alloy 22 in the long transverse-longitudinal (T-L) orientation where the crack plane is perpendicular to the width direction (T direction) and the crack propagation direction is in the rolling longitudinal direction (L direction). Both the DCB and the WOL specimens were wedge loaded using double- tapered wedges whereas the CT specimens were loaded using a testing frame in which a dead weight was applied through a lever arm. In all cases the specimens were fatigue precracked and loaded to the selected stress intensity. Experimental procedures and details have been described elsewhere[72]. Tests were conducted at 95 °C in 0.028 molal NaCl solution, in deaerated 0.9 molal NaCl solution acidified to pH 2.7 by the addition of HCl, and in 9.1 molal LiCl solution, as well as in 9.1 and 14.0 molal Cl^- (as $MgCl_2$) solutions at 110 °C. Whereas several tests were conducted at the E_{corr}, in other tests the potential was controlled potentiostatically at different values. Crack growth in DCB and modified WOL specimens was measured by periodically removing the specimens from the solution and inspecting them with a low magnification optical microscope followed by SEM examination to measure more precisely the advance of the crack. For the CT specimens, crack growth was monitored *in-situ* by performing compliance measurements.

No crack growth was observed in a set of tests conducted with modified WOL specimens of type 316 L SS at initial K_I values of 32.7 and 54.4 MPa·m^{½} after 120 days exposure to the 0.028 molal NaCl solution at 95 °C both under open circuit and anodically applied potentials. Also, no crack growth was observed in a more concentrated chloride solution by using DCB specimens. In this case, the initial K_I was 25.0 MPa·m^{½} and the specimens were exposed to the 0.9 molal NaCl solution (pH 2.7) at 90 °C for 386 days under open circuit conditions. The values of E_{corr} varied from −340 to −320 mV_{SCE} during the test. It is apparent that the test conditions, including chloride concentration, temperature, potential, and initial stress intensity conditions were not conducive to crack growth.

In contrast, substantial crack growth was observed in a DCB specimen tested in 14.0 molal Cl^- (as $MgCl_2$) solution at 110 °C and at the E_{corr} (−320 to −300 mV_{SCE}) after just a 6-day exposure. After 20 days, many transverse cracks, almost perpendicular to the plane of the fatigue precrack, were observed on the arms of the DCB specimen. These transverse cracks released the load applied by the wedge. Hence, a lower initial value of K_I (21.8 MPa·m^{½}) and a less concentrated solution were selected for the following tests with the DCB specimens. The results of these tests conducted in 9.1 molal Cl^- (as $MgCl_2$) solution at 110 °C are plotted in Figure 5. The crack propagation rate, calculated from the crack growth and the time between inspection intervals (without assuming any induction time after immersion of the specimen), is plotted as a function of potential. In addition, Figure 5 also includes the results of tests conducted in 9.1 molal LiCl solution at 95 °C using the modified WOL specimens at initial K_I values of 21.8 and 32.7 MPa·m^{½}. It is seen that the crack growth rates measured with the DCB and WOL specimens exhibited good agreement despite the differences in temperature (~15 °C) and solution pH due to the different degree of hydrolysis of the metal cations used in both set of tests. The rates increased slightly with increasing potential from −380 to −320 mV_{SCE}. However, the most important observation is that no crack growth was detected for both types of specimens, within the limit of resolution of the technique used, below the value of E_{rp} measured in 9.1 molal LiCl solution at 95 °C. By using the optical microscope the lowest

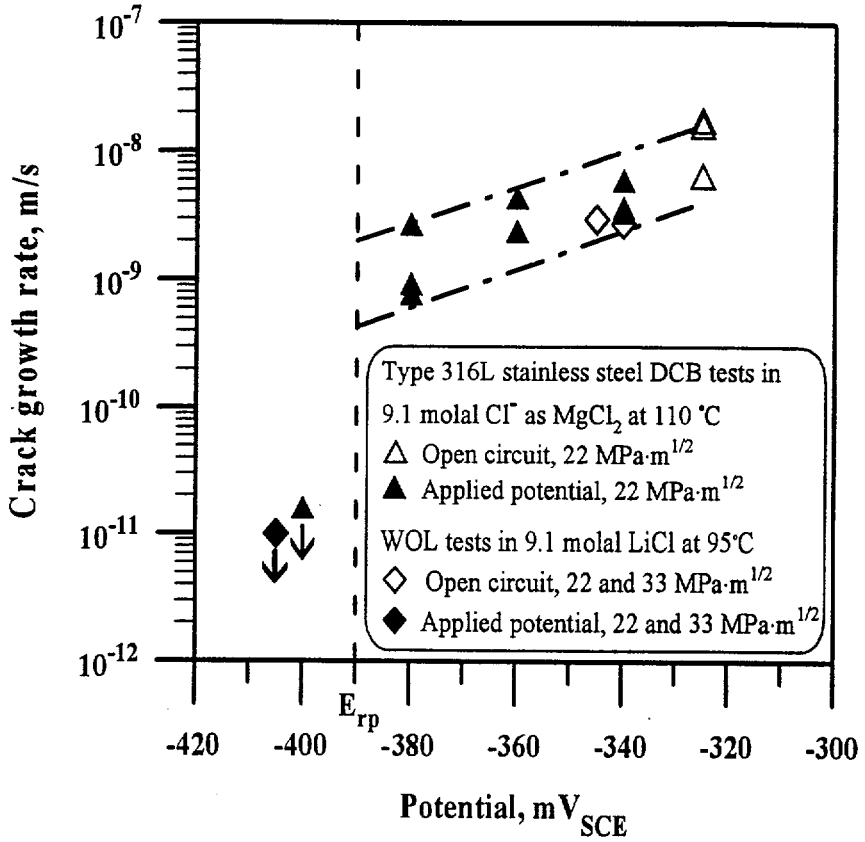

Figure 5: Effect of potential on the crack growth rate of type 316L SS in LiCl and $MgCl_2$ solutions. E_{rp} denotes the repassivation potential for localized corrosion in the LiCl solution.

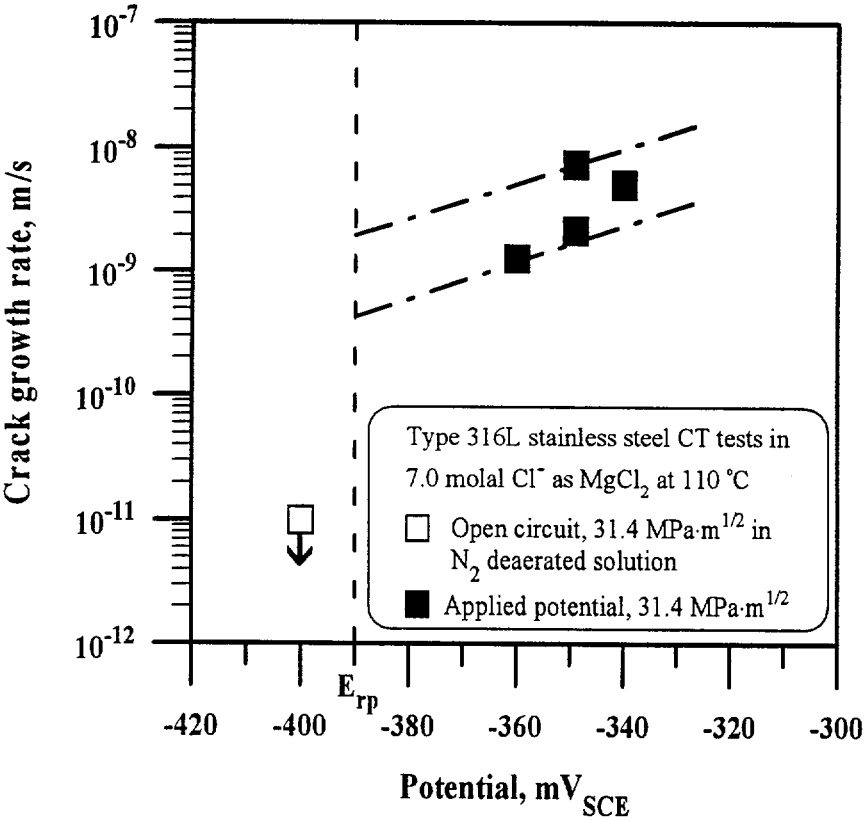

Figure 6: Crack growth rate for CT specimens of type 316L SS in Mg Cl_2 solution in comparison with data for DCB and WOL specimens from Figure 5 indicated as a dashed band

crack growth rate detectable in a 1-month inspection period is 1×10^{-11} m/s. This limit can be lowered by extending the exposure time. Using the DCB specimen tested under open circuit conditions in 9.1 molal Cl^- (as $MgCl_2$) solution at 110 °C, the final equilibrium wedge load was measured once the test was completed and a value corresponding to K_{Iscc} equal to 13.1 MPa·m^{½} was calculated.

The results of measurements of crack growth rate using CT specimens loaded to an initial K_I of 31.4 MPa·m^{½} in 9.1 molal Cl^- (as $MgCl_2$) at 110 °C are shown in Figure 6 in comparison with the data obtained with DCB and WOL specimens, which are shown as a band bounding the data points plotted in Figure 5. It is seen that the crack growth rates are comparable, regardless of the type of specimen, loading method, and differences in the initial K_I. Again, an important observation from these tests is that a specimen under open circuit conditions at potentials lower than E_{rp} did not exhibit crack growth over a test time of 27 days. Another CT specimen was tested in 1.0 molal NaCl solution at 95 °C. No crack growth was observed after a test lasting for 83 days.

Tests were also conducted using DCB specimens of Alloy 22 loaded to an initial K_I equal to 32.7 MPa·m$^{1/2}$. No crack growth was observed in

0.9 molal NaCl solution (pH 2.7) at 90 °C over a cumulative time of 386 days. Assuming a resolution of 10 μm in the SEM examination of fracture surfaces (after the DCB specimen is broken apart), the detection limit is a crack growth rate of 3×10^{-13} m/s. In addition, no crack growth was detected after the same period for either T-L and S-L specimens tested in 14.0 molal Cl^- (as $MgCl_2$) solution at 110 °C under open circuit conditions (E_{corr} ~-280 to -250 mV_{SCE}). Additional details have been provided elsewhere[72].

Discussion

From the experimental results of our own work presented above, as well as from the review of the existing literature, it appears that at least for type 316 L SS and also for others steels of the 300 series, TGSCC occurs over a wide range of concentrations in chloride solutions at temperatures ranging from 80 to 150 °C only within a relatively narrow range of potentials above E_{rp}. The significance of E_{rp} and mechanistic considerations related to initiation and repassivation of localized (pitting and crevice) corrosion were discussed elsewhere[73]. In the case of an open, smooth metal surface, initiation of transgranular cracks requires concentrated chloride solutions and relatively high temperatures. Furthermore, in acidic chloride solutions (e.g., $CaCl_2$, $MgCl_2$) the E_{corr} rests on the range of potentials within which SSs are susceptible to SCC, whereas in more neutral chloride solutions slight anodic polarization or the presence of an oxidant in solution (e.g., $Na_2Cr_2O_7$) seems to be required to initiate cracks. The location of the range of potentials for the chloride-induced SCC of fcc Fe-Cr-Ni alloys, covered by a protective Cr_2O_3-rich passive film, should be distinguished from the active/passive range within which IGSCC of ferritic C-Mn steels occurs. For the Fe-Cr-Ni alloys, localized passivity breakdown above E_{rp} is required for crack initiation, whereas delayed repassivation in the presence of passivating anions (e.g., HCO_3^-/CO_3^{2-}, NO_3^-, OH^-) is postulated to be the cause of crack initiation and propagation for carbon steels[26].

As discussed by Staehle[9,10] and Newman and Mehta[17], if the bulk solutions are extremely acidic (e.g., HCl, Na_2SO_4 + HCl), chloride-induced SCC may occur over specific potential ranges even at ambient temperatures. However, in dilute, neutral chloride solutions, as clearly demonstrated by the work of Tsujikawa and coworkers[20,21,70], nucleation of transgranular cracks requires the existence of an active crevice in which the chloride concentration increases to balance the increase in the concentration of hydrogen ions resulting from the hydrolysis of the metal cations produced by metal dissolution. These concentrated local environmental conditions required to sustain crack nucleation and growth are fulfilled only at potentials above E_{rp}. At even higher potentials, as defined by E_p, generalized pitting or crevice corrosion predominates over the initiation and growth or cracks. The occurrence of TGSCC in nominally dilute chloride solutions, as observed many times in industrial applications of austenitic SSs under heat transfer conditions in occluded regions, can presumably be explained on the basis of these observations.

Chloride concentrations of 9.1 molal or above were necessary in solutions of pH 4 to induce SCC of smooth tensile specimens of type 316 L SS in slow strain rate tests at 95 °C. In addition, as noted above and clearly shown in Figure 2, the potential should be above a critical potential that is close to E_{rp}. SCC also occurred at lower chloride concentrations (6.4 molal) but only in the presence of $Na_2S_2O_3$ (Figure 3). In this case, the potential at which cracking occurred is lower than E_{rp} for the plain chloride solution. As expected, however, it was above that measured in chloride solutions containing thiosulfate. It is well established that thiosulfate activates the localized dissolution of SSs in chloride solutions.

In the constant deflection tests, SCC of type 316L SS was observed at much lower chloride concentration, but only on the specimen surface exposed to the vapor phase. This observation reveals the influence of strong concentration and potential gradients just above the vapor/solution interface on the surface of the

U-bend specimens covered by a thin liquid film in which enhanced transport of oxygen as a cathodic reactant could be a accelerating factor in the open circuit tests. The specific enhancement of the SCC susceptibility in the vapor phase is in general agreement with measurements of K_{ISCC} performed on type 304 SS notched specimens exposed below and above the vapor/solution interface to boiling $MgCl_2$ at 144 °C[74]. In the liquid phase K_{ISCC} was equal to 10 MPa·m^{½}, whereas in the vapor phase decreased to 1.1 MPa·m^{½}. However, the presence of HCl in the vapor phase formed by decomposition of $MgCl_2$ upon heating could be a contributing factor in these results.

The tests conducted with fracture mechanics specimens, both in our own work and in those reported in the literature[21,64], clearly indicate that crack growth for precracked type 316L SS specimens in hot chloride solutions also occurs above a critical potential, as illustrated in Figures 5 and 6. The value of this potential is very close to the range of -380 to -390 mV_{SCE} (-140 to -150 mV_{SHE}) reported by various authors. Above this potential there is a small effect of potential on crack growth rate, but the rate decreases by several orders of magnitude to values below the detection limit (about 1×10^{-11} m/s) at potentials lower than E_{rp}.

On the other hand, alloy 825, due to its higher Ni and Cr contents, is more resistant to the initiation of cracks than type 316L SS as indicated by the lack of SCC in slow strain rate tests using smooth specimens in 9.1 molal LiCl (pH 4) and in 5.8 molal NaCl with the addition of $Na_2S_2O_3$ at 95 °C. These results agree with the findings of Tsujikawa et al.[75]. They reported that alloy 825 did not exhibit SCC in 4.3 molal NaCl solution containing 0.001 to 0.1 M $Na_2S_2O_3$ (pH 4.0) at 80 °C after conducting slow strain rate tests and constant load tests at applied stresses above the yield strength of the alloy. In our work, the presence of an active crevice, where local environmental conditions are sufficiently aggressive in terms of high chloride concentration and low pH, was required to induce SCC in those nominal environments. It is important to note that alloy 825 did not exhibit SCC in the constant deflection tests in concentrated chloride solutions with the exception of 14.0 molal Cl^- (as $MgCl_2$) at 120 °C, a result similar to that of the slow strain rate tests using smooth specimens. No fracture mechanics tests were conducted using alloy 825. Due to the limited data available, it is difficult to conclude whether a critical potential can be identified within the ranges of temperatures and chloride concentrations studied.

Similarly, there is no possibility of evaluating the validity of the critical potential concept on the basis of the fracture mechanics tests in the case of alloy 22 because of the lack of crack growth under the environmental conditions tested. Following the trend of the Copson's curve, as reevaluated by Speidel[60] using WOL specimens, both alloys 825 and 22 should exhibit, as a result of their high Ni contents, values of K_{ISCC} at least as high as 60 MPa·m^{½} in 4.8 molal NaCl solution at 105 °C. As discussed above, a criterion based on K_{ISCC} can be used to provide a framework for assessing the SCC susceptibility by assuming that for K_I values below K_{ISCC} preexisting cracks will not propagate or actively growing cracks will be arrested. As noted, however, K_{ISCC} was defined by Speidel[60] for a minimum crack growth rate of 3×10^{-11} m/s. Hence, it is possible that crack growth may occur at rates lower than this limit. The rates at K_I values lower than the "pseudo" K_{ISCC} may be obtained by extrapolation of Eq. (17). However, if a change in the crack growth mechanism occurs, a second plateau may exist with crack growth rates that can be acceptable for many applications but not for performance periods extended over several hundred or thousand years.

In this context, there are two aspects that need additional discussion. The first refers to the existence of the critical potential as an absolute limit for the nucleation and growth of stress corrosion cracks. From our own work and the literature data reviewed above, it appears that a critical potential exists for the case of the TGSCC of austenitic SS in hot, concentrated chloride solutions. However, Galvele and

coworkers[53,76] have shown using slow strain rate tests that for type 304 SS there is a range of potentials of about 100 mV below the TGSCC critical potential within which IGSCC was observed at temperatures above 80 °C in both LiCl and freshly prepared $MgCl_2$ solutions. This intergranular cracking range was not predictable from potentiostatic straining electrode tests and it was attributed to the specific influence of impurity segregation to grain boundaries as no indication of sensitization resulting from chromium carbide precipitation and concurrent chromium depletion was observed[53]. IGSCC was no longer observed when the concentrated $MgCl_2$ solution was aged or boiled and then HCl was released with the concurrent increase in the solution pH. Regardless of the existence of IGSCC in other austenitic SSs or in more neutral environments, a significant decrease in crack velocity, not fully quantified yet but at least about two orders of magnitude, should be expected below the "critical" potential.

The second aspect refers to the applicability of the mechanistic interpretations and models reviewed above. In the slip dissolution/film rupture model, there is no provision to account for discontinuities in the crack velocity versus potential or applied stress (or stress intensity) plots derived from Eqs. (7), (11) and (12). As a consequence, a slow decrease of crack growth rate with decreasing potential or stress intensity is predicted. In the film-induced cleavage model, there is no explicit or implicit dependence of crack velocity with potential. Although the surface mobility model has not been applied from this point of view to the chloride-induced cracking of austenitic SSs, it was used to predict the existence of a critical potential above which crack nucleation and growth can occur for the SCC of Ag-15Pd alloy in various halides and sulfate solutions[54]. The critical potential was found for the Ag-Pd alloy to be the equilibrium electrode potential for the formation of AgCl, AgBr, AgI, and Ag_2SO_4 assumed to be the constituents of the surface film responsible for the enhanced mobility of ad-atoms and vacancies. The surface mobility model was applied to the SCC of type 304 SS in concentrated chloride solutions[16] using data reported by Speidel[60]. The increase in crack velocity with temperature from 25 to 130 °C was fitted to the model predictions using the measured crack grow rate at a single temperature. Unfortunately, although good agreement was observed between experiment and theory, most of the data points reported by Speidel[60] correspond to the SCC of the sensitized alloy, in which a preexisting susceptible path exists and thus anodic dissolution is the cause of crack advance.

There is an additional problem regarding the applicability of the models discussed above to predict the mechanical and environmental conditions for the occurrence of SCC and the time to failure according to Eqs. (1) and (2). As noted, all these models deal only with the crack propagation stage and hence, the initiation time, which usually is the most important contribution to the failure time, cannot be accounted for. This predominant influence of crack initiation, and other considerations regarding SCC modeling, led Staehle[77] to develop a systematic approach for the prediction of SCC in which statistical considerations are emphasized. If the existence of the critical potential in chloride solutions is verified for other Fe-Cr-Ni alloys with Ni contents below 42 %, the type of probability distribution and the range of values for the critical potential can be related to the equivalent distributions for E_{rp}[73].

Summary and Conclusions

The existence of a critical potential for the TGSCC of fcc Fe-Cr-Ni-Mo alloys in hot chloride solutions below which crack initiation does not occur was discussed based on data reported in the literature and on our own work using several experimental techniques that include slow strain rate, constant deflection and fracture mechanics tests with DCB, modified WOL, and CT specimens. Using data obtained from slow strain rate and constant deflection tests, it appears that the SCC critical potential coincides with the E_{rp} for crevice corrosion for type 316 SS in hot, dilute chloride solutions. On the basis of this concept, the

approach for predicting the environmental conditions for the occurrence of SCC in many industrial applications is similar to that described for localized corrosion in the form of crevice corrosion.

The possibility of using K_{Iscc} as an additional threshold parameter was discussed, emphasizing the influence of environmental conditions and potential in the value of this parameter. K_{Iscc} values ranging from approximately 8 to 20 MPa·m$^{1/2}$ have been observed for types 304, 304L, 316, and other similar austenitic SSs in chloride-containing solutions at temperatures ranging from 80 to 130 °C, whereas values higher than 60 MPa·m$^{1/2}$ have been reported for Fe-Cr-Ni-Mo alloys with Ni contents higher than 40 percent. As expected, the values in the lower end of the range for the SSs of the 300 series are those observed with both increasing temperatures and chloride concentration. Because K_{Iscc} is defined in terms of a limiting crack growth rate as a result of the experimental difficulties encountered in measuring rates below 1×10^{-11} m/s, its validity as a predictive parameter for long-term performance assessment should be based on an appropriate combination of experimental and modeling work.

Although it is recognized that SCC initiation models are more important than propagation models for the time scales of interest in certain applications (e.g., high-level radioactive waste disposal), most of the existing models refer to propagation. One of the main limitations in several of these models is the lack of appropriate data to establish the value of the parameters needed for predictive purposes.

Acknowledgments

This paper was prepared to document work performed by the CNWRA for the U.S. Nuclear Regulatory Commission (NRC) under contract No. NRC-02-97-009. This paper is an independent product of the CNWRA and does not necessarily reflects the views or regulatory position of the NRC.

References

1. Uhlig, H.H. and E.W. Cook, Jr., Journal of the Electrochemical Society, 116 (1969), 173.

2. Lee, H.H. and H.H. Uhlig, Journal of the Electrochemical Society 117 (1970), 18–22.

3. Hines, J.G. and T.P. Hoar, Journal of Applied Chemistry. London, England, 8 (1958), 764–776.

4. Brennert, S., Jernkontorets Annaler 144 (1960), 560–566.

5. Barnartt, S,, and D. van Rooyen, Journal of the Electrochemical Society 108 (1961), 222–229.

6. Smialowski, M. and M. Rychik, Corrosion, 23 (1967), 218–221.

7. Uhlig, H.H. in Stress Corrosion Cracking and Hydrogen Embrittlement of Iron Base Alloys R.W. Staehle, J. Hochmann, R.D. McCright, and J.E. Slater, eds. (Houston, TX: National Association of Corrosion Engineers 1977), 174–179.

8. Uhlig, H.H. Journal of Applied Electrochemistry 9 (1979), 191–199.

9. Staehle, R.W., in Theory of Stress Corrosion Cracking in Alloys J.C. Scully, ed. (Brussels: North Atlantic Treaty Organization, 1971), 223–288.

10. Staehle, R.W., in Stress Corrosion Cracking and Hydrogen Embrittlement of Iron Base Alloys, R.W. Staehle, J. Hochmann, R.D. McCright, and J.E. Slater, eds. (Houston, TX: National Association of Corrosion Engineers, 1977), 180–207.

11. Latanision, R.M. and R.W. Staehle, in Fundamental Aspects of Stress Corrosion Cracking R.W. Staehle, A.J. Forty, and D.van Rooyen, eds. (Houston, TX: National Association of Corrosion Engineers, 1969), 214–307.

12. Theus, G..J. and R.W. Staehle, in Stress Corrosion Cracking and Hydrogen Embrittlement of Iron Base Alloys R.W. Staehle, J. Hochmann, R.D. McCright, and J.E. Slater, eds. (Houston, TX: National Association of Corrosion Engineers, 1977), 845–892.

13. Ford, F.P., in Treatise on Materials Science and Technology. Vol. 25. Embrittlement of Engineering Alloys C.L. Briant and S.K. Banerji, eds. New York, NY: (Academic Press, 1983), 235–274.

14. Ford, F.P., and P.L. Andresen, in Proceedings of the Third International Symposium on Environmental Degradation of Materials in Nuclear Power Systems-Water Reactors G.J. Theus and J.R. Weeks, eds. (Warrendale, PA: The Metallurgical Society, 1988), 789–800.

15. Sieradzki, K., and R.C. Newman, Philosophical Magazine A 51, (1985), 95–132.

16. Galvele, J.R., Corrosion Science 27, (1987), 1–33.

17. Newman, R.C. and A. Mehta, in Environment-Induced Cracking of Metals R.P. Gangloff and M.B. Ives. (Houston, TX: National Association of Corrosion Engineers, 1990), 489–509.

18. Sedriks, A.J., in Stress-Corrosion Cracking. Materials Performance and Evaluation R.H. Jones, ed. (Materials Park, OH: ASM International, 1992), 91–130.

19. Cragnolino, G.A., and N. Sridhar, A Review of Stress Corrosion Cracking of High-Level Nuclear Waste Container Materials—I CNWRA 92-021. (San Antonio, TX: Center for Nuclear Waste Regulatory Analyses, 1992).

20. Tsujikawa, S., T. Shinihara, and Y. Hisamatsu, in Corrosion Cracking V.S. Goel, ed. (Metals Park, OH: American Society for Metals, 1985), 35–42.

21. Tamaki, K., S. Tsujikawa, and Y. Hisamatsu. in Advances in Localized Corrosion H.S. Isaacs, U. Bertocci, J. Kruger, and S. Smialowska, eds. (Houston, TX: National Association of Corrosion Engineers, 1990), 207–214.

22. Hagn, L., in Corrosion in Power Generating Equipment M.O. Speidel and A. Atrens, eds. (New York, NY: Plenum Press, 1984), 481–516.

23. Ranjan, R., and O. Buck, in Predictive Capabilities in Environmentally Assisted Cracking R. Rungta, ed. (New York, NY, PVP-Vol. 99, The American Society of Mechanical Engineers, 1985), 79–89.

24. Buck, O., and R. Ranjan, in Modeling Environmental Effects on Crack Growth Processes R.H. Jones and W.W. Gerberich, eds. (Warrendale, PA: The Metallurgical Society, 1986), 209–223.

25. Parkins, R.N. British Corrosion Journal 7, (1972), 15–28.

26. Parkins, R.N. in Environment-Induced Cracking of Metals. R.P. Gangloff and M.B. Ives, eds. (Houston, TX: National Association of Corrosion Engineers 1990), 1–29.

27. Jones, R.H., and R.E. Ricker. in Stress-Corrosion Cracking. Materials Performance and Evaluation. R.H. Jones, ed. (Materials Park, OH: ASM International, 1992), 1–40.

28. Beck, T.R. Corrosion 30, (1974), 408–414.

29. Beck, T.R. in Electrochemical Techniques for Corrosion. R. Baboian, ed. (Houston, TX: National Association of Corrosion Engineers, 1977), 27–34.

30. Newman, R.C. in Corrosion Chemistry within Pits, Crevices and Cracks. A. Turnbull, ed. (Teddington, U.K.: Her Majesty's Stationary Office, 1987), 317–356.

31. Turnbull, A., and M. Psaila-Dombrowski. Corrosion Science 33, (1992), 1,925–1,966.

32. Forty, A.J., and P. Humble. Philosophical Magazine 8, (1963), 247–253.

33. McEvily, A.J., and A.P. Bond. Journal of the Electrochemical Society 112, (1965), 131–138.

34. Vermilyea, D.A. Journal of the Electrochemical Society 119, (1972), 405–407.

35. Vermilyea, D.A. in Stress Corrosion Cracking and Hydrogen Embrittlement of Iron Base Alloys. R.W. Staehle, J. Hochmann, R.D. McCright, and J.E. Slater, eds. (Houston, TX: National Association of Corrosion Engineers, 1977), 208–217.

36. Scully, J.C. Corrosion Science 15, (1975), 207–224.

37. Newman, J.F. Corrosion Science 21, (1981), 487–503.

38. Ford, F.P., and P.L. Andresen. in. Parkins Symposium on Fundamental Aspects of Stress Corrosion Cracking. S.M. Bruemmer, E.I. Meletis, R.H. Jones, W.W. Gerberich, F.P. Ford, and R.W. Staehle, eds. (Warrendale, PA: The Minerals, Metals, and Materials Society, 1992) 43–67.

39. Ford, F.P., and P.L. Andresen. The theoretical prediction of the effect of system variables on the cracking of stainless steel and its use in design. *CORROSION/87*. Paper No. 83. (Houston, TX: National Association of Corrosion Engineers, 1987).

40. Lidbury, D.P.G. in Embrittlement by the Localized Crack Environment. R.P. Gangloff, ed. (Warrendale, PA: The Metallurgical Society, 1984), 149–172.

41. Parkins, R.N. Factors influencing stress corrosion crack growth kinetics. *CORROSION/87*. Paper No. 177. (Houston, TX: National Association of Corrosion Engineers, 1987).

42. Ford, F.P. in Environment-Induced Cracking of Metals. R.P. Gangloff and M.B. Ives, eds. (Houston, TX: National Association of Corrosion Engineers, 1990), 139–165.

43. Macdonald, D.D., and M. Urquidi-Macdonald. Corrosion Science 32, (1991), 51–61.

44. Macdonald, D.D., and M. Urquidi-Macdonald. in Proceedings of the Fifth International Symposium on Environmental Degradation of Materials in Nuclear Power Systems—Water Reactors. D. Cubicciotti and E.P. Simonen, eds. (La Grange Park, IL: American Nuclear Society, 1992), 345–349.

45. Macdonald, D.D., Corrosion Science 38, (1996), 1,003–1010.

46. Andresen, P.L., and F.P. Ford. Corrosion Science 38, (1996) 1,011–1,016.

47. Macdonald, D.D., Corrosion Science 39, (1997), 1,487–1,490.

48. Macdonald, D.D., P-C.W. Lu, M. Urquidi-Macdonald, and T.-K.Yeh, Corrosion 52, (1996), 768–785.

49. Pugh, E.N. Corrosion 41, (1985), 517–526.

50. Turnbull, A. Corrosion Science 34, (1993), 921–960.

51. Cole, A.T., R.C. Newman, and K. Sieradzki. Corrosion Science 28, (1988), 109–118.

52. Galvele, J.R. .in Parkins Symposium on Fundamental Aspects of Stress Corrosion Cracking. S.M. Bruemmer, E.I. Meletis, R.H. Jones, W.W. Gerberich, F.P. Ford, and R.W. Staehle, eds. (Warrendale, PA: The Minerals, Metals, and Materials Society, 1992), 85–101.

53. Duffó, G.S., I.A. Maier, and J.R. Galvele. Corrosion Science 28, (1988), 1,003–1,018.

54 Duffó, G.S., and J.R. Galvele. Corrosion Science 30, (1990), 249–257.

55. Galvele, J.R. in Modern Aspects of Electrochemistry. J.O'M. Bockris, B.E. Conway, and R. White, eds. (New York, Plenum Press, 1995), Vol. 27: 233–285.

56. Galvele, J.R. Electrochimica Acta 45, (2000), 3,537–3,541.

57. Brown, B.F. Metallurgical Reviews 13, (1968), 171–183.

58. Speidel, M.O. in Theory of Stress Corrosion Cracking in Alloys. J.C. Scully, ed. (Brussels, Belgium: North American Treaty Organization, 1971), 289–344.

59. Jones, R.H., and E.P. Simonen. Materials Science and Engineering *A* 160 (1993), 127–136.

60. Speidel, M.O. Metallurgical Transactions *A* 12, (1981) 779–789.

61. Komai, K, K. Minoshima, and T. Miyawaki, Journal de Physique IV Colloque C6. Vol. 6: C6-413-420. 1996.

62. Blackburn, M.J., W.H. Smyrl, and J.A. Feeney., in Stress-Corrosion Cracking in High Strength Steels and in Titanium and Aluminum Alloys. B.F. Brown, ed. (Washington, DC: Naval Research Laboratory, 1972), 245–363.

63. Oelkers, E.H., and G.C. Helgeson. Geochimica et Cosmochimica Acta 52, (1988), 63–85.

64. Russell, A.J., and D. Tromans. Metallurgical Transactions *A* 10, (1979), 1,229–1,238.

65. Feeney, J.A., and M.J. Blackburn., in Theory of Stress Corrosion Cracking in Alloys. J.C. Scully, ed. (Brussels, Belgium: North American Treaty Organization, 1971), 355–398.

66. Eremias, B., and V.V. Marichev. Corrosion Science 20, (1980), 307–312.

67. Silcock, J.M. Corrosion 38, (1982), 144–156.

68. Shamakian, R.L., A.R. Troiano, and R.F. Heheman., in Environment-Sensitive Fracture of Engineering Materials. Z.A. Foroulis, ed. (Warrendale, PA: TMS, 1979), 116–132.

69. Shamakian, R.L., A.R. Troiano, and R.F. Heheman. Corrosion 36, (1980), 279–284.

70. Tsujikawa, S., T. Shinohara, and W. Lichang., in Applications of Accelerated Corrosion Tests to Service Life Prediction of Materials. G. Cragnolino and N. Sridhar, eds. ASTM STP 1194. (Philadelphia, PA: American Society for Testing and Materials, 1994), 340–354.

71. Cragnolino, G.A., D.S. Dunn, and N. Sridhar. Corrosion 52, (1996), 194–203.

72. Pan, Y.-M., D.S. Dunn, and G.A. Cragnolino., in Environmentally Assisted Cracking: Predictive Methods for Risk Assessment and Evaluation of Materials, Equipment, and Structures. ASTM STP 1401. R.D. Kane, ed. (West Conshohocken, PA: American Society for Testing and Materials, 2000), 273–288.

73. Dunn, D.S., G.A. Cragnolino, and N. Sridhar, Corrosion 56, (2000), 90–104.

74. Lefakis, H., and W. Rostoker. Corrosion 33, (1977), 178–181.

75. Tsujikawa, S., A. Miyasaka, M. Uedo, S. Ando, T. Shibata, T. Haruna, M. Katahira, Y. Yamane, T. Aoki, and T. Yamada. Corrosion 49, (1993), 409–419.

76. Manfredi, C., I.A. Maier, and J.R. Galvele. Corrosion Science 27, (1987), 887–903.

77. Staehle, R.W., in Environmentally Assisted Cracking: Predictive Methods for Risk Assessment and Evaluation of Materials, Equipment and Structures. ASTM STP 1401. R.D. Kane, ed. (West Conshohocken, PA: American Society for Testing and Materials, 2000), 131–165.